Thermal evolution of Tethyan surface waters during the Middle-Late Jurassic: Evidence from $\delta^{18}O$ values of marine fish teeth

Christophe Lécuyer,[1,2] Stéphanie Picard,[1] Jean-Pierre Garcia,[3] Simon M. F. Sheppard,[4] Patricia Grandjean,[1] and Gilles Dromart[1]

Received 9 November 2002; revised 27 March 2003; accepted 16 May 2003; published 25 September 2003.

[1] Oxygen isotope compositions of phosphate from vertebrate tooth enamel were measured to determine the evolution of tropical sea surface (<~200 m depth) temperatures in the western Tethys during the Middle-Late Jurassic. On the basis of a high-resolution stratigraphic framework with a 1 Myr time resolution, vertebrate teeth were sampled on Aalenian to Portlandian isochrons over the Anglo-Paris Basin. *Asteracanthus* sharks and Pycnodontidae teleosteans, identified as sea surface dwellers, have enamel with $\delta^{18}O$ values that range from 18.5 to 22.3‰. Thermal variations of tropical surface waters, with amplitudes of a few degrees per few million years, suggest that Middle to Late Jurassic climates were quite variable. Assuming a seawater $\delta^{18}O$ value of 0‰ for surface tropical waters in the absence of polar ice caps, temperatures increased from 25 to 29°C from the mid-Bajocian to mid-Bathonian. During the middle to late Bathonian, a strong geographic zonation in isotopic compositions is observed between the eastern and western parts of the basin. High $\delta^{18}O$ values of fish tooth enamel (up to 22.3‰) could reflect the arrival of a cold water current from the Arctic during the opening of the North Sea rift. An apparent large drop of temperatures from 28 to 21°C is identified at the Callovian-Oxfordian boundary over no more than ≈2–3 Myr. This cooling is compatible with previous paleobotanical and geochemical studies and can be precisely correlated with the migration of boreal ammonites into the Tethyan domain. Because isotopic sea surface temperatures are probably too low to be compatible with tropical climatic conditions, the $\delta^{18}O$ value of seawater could have been >0‰ owing to limited growth of continental ice during the early middle Oxfordian. The resulting sea level fall is estimated to be at least 50 m and is compatible with a global regression stage. The middle Oxfordian thermal minimum is followed by a new warming stage of 3–4°C from the middle to the late Oxfordian. *INDEX TERMS:* 1040 Geochemistry: Isotopic composition/chemistry; 1045 Geochemistry: Low-temperature geochemistry; 1620 Global Change: Climate dynamics (3309); *KEYWORDS:* oxygen isotope, phosphate, shark, Jurassic, seawater, climate

Citation: Lécuyer, C., S. Picard, J.-P. Garcia, S. M. F. Sheppard, P. Grandjean, and G. Dromart, Thermal evolution of Tethyan surface waters during the Middle-Late Jurassic: Evidence from $\delta^{18}O$ values of marine fish teeth, *Paleoceanography*, *18*(3), 1076, doi:10.1029/2002PA000863, 2003.

1. Introduction

[2] The Jurassic has long been considered to have been a warm and equable period of Earth history, based on floral and faunal distribution patterns [e.g., *Frakes and Francis*, 1990; *Frakes et al.*, 1992; *Hallam*, 1998]. However, recent paleobotanical [e.g., *Philippe and Thévenard*, 1996; *Hubbard and Boulter*, 1997; *Morgans et al.*, 1999; *Riding and Hubbard*, 1999; *Van Aarssen et al.*, 2000] and oxygen isotope studies on belemnites and brachiopods [e.g., *Ditchfield*, 1997; *Veizer et al.*, 1997; *Podlaha et al.*, 1998; *Riboulleau et al.*, 1998] have provided evidence for fluctuations of both paleotemperatures and humidity during the Jurassic. Continuous paleoclimatic curves, however, cannot be established from the limited, and fragmentary database of samples from variable water depths.

[3] Fossil biogenic apatite, especially enamel, shows more resistance than carbonate shells to oxygen isotope exchange during diagenesis [*Kolodny et al.*, 1983; *Kolodny and Raab*, 1988; *Lécuyer et al.*, 1993]. Biogenic apatites, that crystallize in apparent equilibrium with seawater, have $\delta^{18}O$ values that are fixed by the temperature and the isotopic composition of water [*Longinelli and Nuti*, 1973; *Kolodny et al.*, 1983]. Empirical fractionation equations have been determined with present-day invertebrate and vertebrate ectotherms, leading to a single temperature-dependent curve [*Longinelli and Nuti*, 1973; *Kolodny et al.*, 1983; *Lécuyer et al.*, 1996a]. This intrinsic property of the phosphate oxygen-water system can be applied to extinct species to derive past temperatures, assuming a $\delta^{18}O$ value for the environmental water. The oxygen isotope composition of well-preserved biogenic apatites has already been successfully used as a marine paleothermometer [*Kolodny*

[1]Laboratoire Paléoenvironnements et Paléobiosphère UMR CNRS 5125, Centre Nationale de Recherche Scientifique, Campus de la Doua, Université Claude Bernard Lyon 1, Villeurbanne, France.
[2]Also at Institut Universitaire de France, Paris, France.
[3]Centre des Sciences de la Terre, Centre Nationale de Recherche Scientifique, Université de Bourgogne, Dijon, France.
[4]Laboratoire de Sciences de la Terre, Centre Nationale de Recherche Scientifique, Ecole Normale Supérieure de Lyon, Lyon, France.

Copyright 2003 by the American Geophysical Union.
0883-8305/03/2002PA000863$12.00

and Raab, 1988; *Kolodny and Luz*, 1991; *Lécuyer et al.*, 1993, 1996b; *Picard et al.*, 1998; *Vennemann and Hegner*, 1998].

[4] Before the Latest Jurassic-Early Cretaceous radiation of carbonate plankton [*Roth*, 1989], ectotherm vertebrates living in surface waters, defined here as about the top 100 m of the water column, can be considered as potential substitutes of paleorecorders of sea surface temperatures [*Picard et al.*, 1998]. To characterize the living depth of Jurassic fish, their $\delta^{18}O$ values were compared with a previously obtained data set of coexisting brachiopods [*Picard et al.*, 1998]. The oxygen isotope compositions of brachiopods record bottom-water temperatures from the shallowest to the deepest depositional environments of the Anglo-Paris Basin. The oxygen isotope compositions of brachiopods appeared to be in good agreement with independent hydrodynamic and sedimentary criteria [*Guillocheau*, 1991].

[5] Well documented sedimentological and paleogeographic studies of the 600 km $\times$ 800 km Anglo-Paris Basin [*Ziegler*, 1988; *Guillocheau*, 1991; *Robin et al.*, 2000] and the high-resolution stratigraphic framework, set up by *Garcia et al.* [1996], *Gaumet et al.* [1996] and *Garcia and Dromart* [1997], may help us to understand changes in the hydrologic budget and oceanic circulation patterns that affected its water masses. This Basin was located at tropical latitudes (20°–30°N) during the Middle and Late Jurassic [*Dercourt et al.*, 1985; *Ziegler*, 1988] with water depths down to about 200 m [*Guillocheau*, 1991; *Picard et al.*, 1998]. This epicontinental sea, representing the occidental part of the equatorial Tethyan ocean, was connected to the opening central Atlantic ocean. Since the middle Bathonian, the development of seaways to the north probably enabled efficient communication of surface waters between the Tethyan Basin and boreal realms.

[6] The Anglo-Paris Basin, with its high-resolution stratigraphic framework, thus constitutes an especially interesting case study to apply oxygen isotope compositions of Middle to Late Jurassic fish tooth enamel to (1) reconstruct tropical surface seawater temperature variations with time, (2) document the existence of paleocurrents and their influence on faunal migration at the few million year timescale, and (3) explore the consequences of tropical temperature variations in terms of sea level variations and the possible presence of a polar ice cap.

2. Depositional Environments

[7] Depositional environments were dominated by three main carbonate platform domains (Burgundy, Ardennes and Normandy), Normandy being separated from the two others by a marly furrow and bordered by land masses during the Bathonian and the middle and late Oxfordian (Figure 1). The Callovian is characterized by the drowning of relatively high areas by clayey and sandy wedges with a maximum flooding surface in the middle Callovian [*Gaumet et al.*, 1996]. A regressive-transgressive second-order sequence was recorded in the late Bajocian to middle Callovian carbonate series [*Guillocheau*, 1991; *Garcia et al.*, 1996]. This sequence includes (1) a regressive hemicycle from the upper Bajocian to the lower-middle Bathonian boundary corresponding to an overall infill of the basin by progradation of carbonate platforms until subaerial exposure, and (2) a transgressive hemicycle from the middle Bathonian until the transgressive peak of middle Callovian age (Jason zone). Siliciclastic sands and silts were deposited at the same time in southern England and over the Channel (between England and France). The next regressive-transgressive cycle corresponds to the progradation of siliciclastic (middle Callovian to middle Oxfordian) then carbonate wedges from northwest to southeast.

[8] The water depth of the fair weather and storm wave limits may fluctuate depending on both coastal morphology and occurrence of submarine topographic breaks. Nonetheless, these hydrodynamic parameters can be used to define four main depositional environments in the Anglo-Paris basin. (1) The protected environment where wave action is limited by topographic barriers. These environments can sometimes correspond to relatively deep locations compared to emersive lagoonal environments. Shallow environments show evidence of limited subaerial exposure such as mud cracks or birds' eyes, but without evaporites (excluding dolomite) or significant siliciclastics. (2) The shoreface above the fair weather wave base forms barriers that were oolitic and skeletal in the Bathonian and Callovian, and were often made up of reefal mounds in the Oxfordian. (3) The upper offshore located between the fair weather and the storm wave bases, and (4) the lower offshore occurs below the storm wave base.

3. Sample Collection

[9] Eighty nine teeth (including seventy eight enamels and eleven whole teeth) and two bones of Chondrichtyan and Osteichtyan Jurassic fish were selected from shallow to deep marine environments of the Anglo-Paris Basin (Table 1; Figure 1). In addition, eleven bulk teeth and one tooth enamel of reptiles, mainly marine crocodilians, were selected when found associated with fish teeth. Vertebrate remains were sampled along sedimentary isochron profiles [*Garcia et al.*, 1996; *Gaumet et al.*, 1996] with a resolution of about 1 Myr from the Bajocian to the Tithonian, with one Aalenian tooth. Isochrons consist of sedimentary beds defined by monospecific or plurispecific brachiopod associations that are laterally continuous throughout the basin and coincide with maximum platform floodings [*Garcia and Dromart*, 1997]. These brachiopod shell beds were accurately identified on the basis of one hundred and forty exploratory oil wells that were used to construct high frequency cycle correlations [*Garcia and Dromart*, 1997]. They were also calibrated with ammonite standard zonation and Jurassic timescale [*Gradstein et al.*, 1994].

[10] Chondrichtyan fish are sharks represented by four main genera that are *Asteracanthus* (crushing fish), *Notidanus*, *Sphenodus* and *Odontaspis* (tearing fish). *Asteracanthus* feeds on shells and is characterized by platy and massive teeth with an enamel structure [*Cuny*, 1998]. Jurassic Osteichtyan fish are represented by durophageous fish, Pycnodontidae with tabular teeth, except one genus, *Sphaerodus*, having hemispherical teeth, and Gyrodontidae (*Gyrodus*). Ecology and, especially, living depths of Jurassic fish, cannot simply be determined from paleontological or paleoenvironmental criteria. Depositional environments,

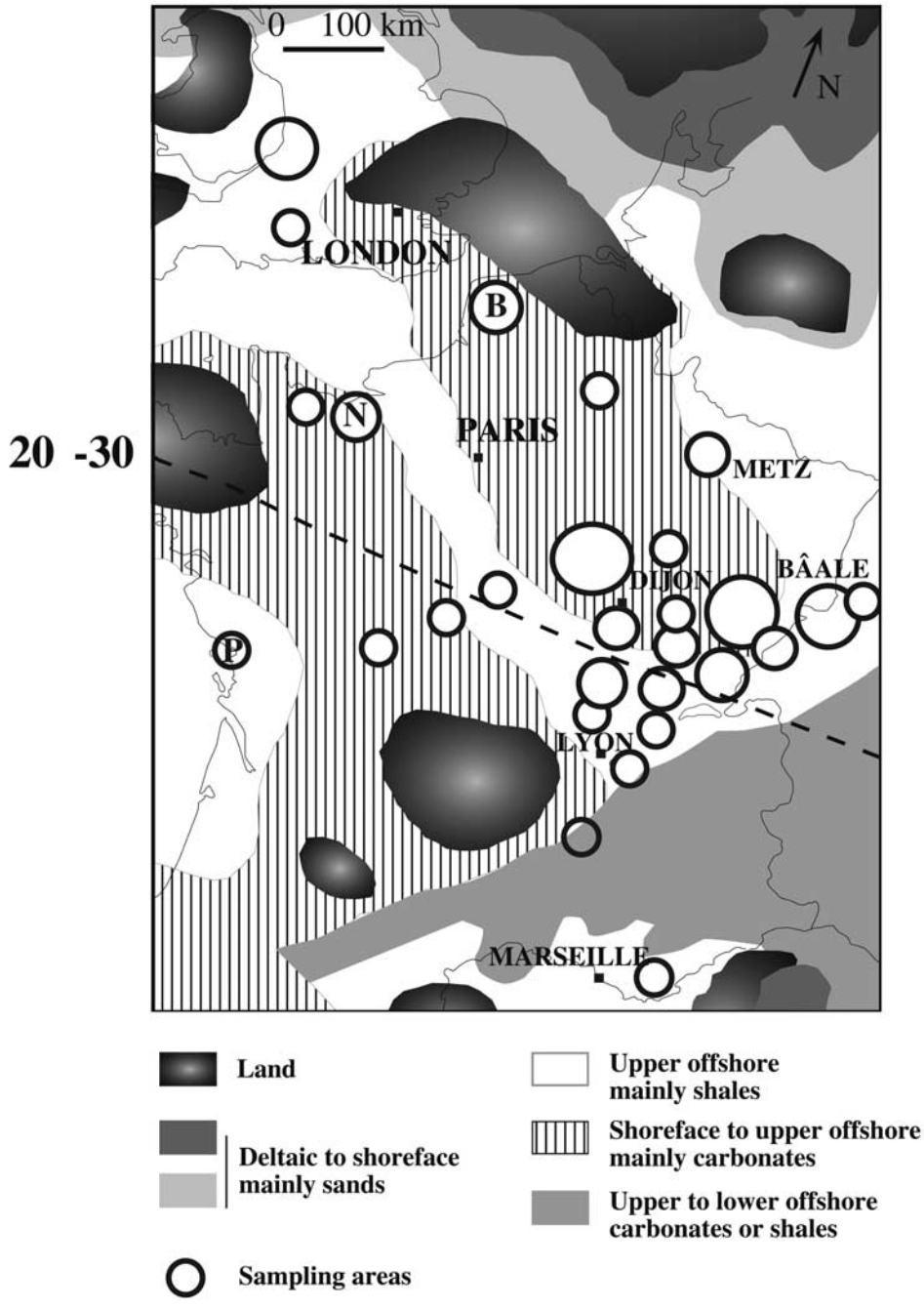

Figure 1. Sampling locations of Jurassic fish and reptile remains. The size of open circles is proportional to the number of sites. Biogenic phosphates were selected from the western (Normandy, Boulonnais, south England) and the eastern (Burgundy, Jura, and southeast basin) parts of the Anglo-Paris Basin. The paleogeographic map (modified after *Dercourt et al.* [1985] and *Ziegler* [1988]) shows that Western Europe occupied a tropical position during the Middle-Late Jurassic; a latitude is shown and labelled 20°–30° to give an estimate of uncertainties. Since the Bathonian, the Anglo-Paris basin, located at the occidental extremity of the Tethys, was connected northward to boreal realms. North-south seaways, formed during the initial rifting phases of the North Sea, were generally filled by shallow marine (early-middle Bathonian), then by deeper marine deposits (late Bathonian). Abbreviations are as follows: B, Boulonnais; N, Normandy; P, Poitou.

Table 1. Oxygen Isotope Compositions of Aalenian to Portlandian Vertebrate Phosphates Along With Taxon Determination, Sample Locations, Ages, and Environments[a]

Vertebrate Taxa	Code	Sample	Stratigraphic Age	Ammonite Zones	Isochron	Age, Myr		Location	Depositional Environments	$\delta^{18}O$, ‰	P_2O_5, %
Odontapsis	93399	T-e	Aalenian	Concavum	Concavum	177.1	Cu	Hte Saône-Coulevon	O	19.3	43
Asteracanthus	D66[b]	T-e	E. Bajocian	Sauzei	Sauzei	174.3	St	Var-Solliès-Toucas	UO	18.7	41
Pycnodus	L9[b]	T-e	M. Bajocian	Humphriesianum	Humphriesianum	173.2	Se	Saône et Loire-Sennecey	UOPZ	20.5	44
Oxyrhina	L12	T-b	M. to L. Bajocian	Humphriesianum	Humphriesianum	172	Li	Saône et Loire-St Sorlin	UOPZ	19.5	37
Pycnodus	93401[b]	T-e	M. Bajocian	Humphriesianum	Humphriesianum	172	Li	Saône et Loire-Laives	UOPZ	19.9	44
Fish	D28	B	L. Bajocian	Acris	Acris	170.2	Po	Côte d'Or-Pouillenay	UOpPZ	14	28
Asteracanthus	L10[b]	T-e	L. Bajocian	Acris	Acris	170.2	H	Saône et Loire-Hurigny	UOBPZ	20.1	34
Marine reptile	L11	T-b	L. Bajocian	Acris	Acris	170.2	H	Saône et Loire-Hurigny	UOBPZ	17.5	30
Hybodus	O1	T-b	L. Bajocian	Parkinsoni	Parkinsoni	169.3	O	Calvados-Omaha beach	UO	21.2	29
Pycnodont	D111-p[b]	T-e	E. Bathonian	Convergens	Convergens	169.1	Bn	Var-Bandol	UO	19.7	38
Asteracanthus	93357[b]	T-e	E.-M. Bathonian	Progracilis	Globata	167.9	S	Stonesfield (UK)	P	20.5	33
Crocodylian	93369	T-b	E.-M. Bathonian	Progracilis	Globata	167.9	S	Stonesfield (UK)	P	20.8	28
Asteracanthus	D109-A[b]	T-e	E.-M. Bathonian	-	-	-	Vy	Cher-Vallenay	S	19.4	42
Asteracanthus	AST 53[b]	T-e	E.-M. Bathonian	Progracilis-Subcontractus	Globata-Multiplicata	167.9	Me	Jura-Merey s/Montrond	P	18.7	35
Asteracanthus[c]	D6[b]	T-e	M. Bathonian	Progracilis-Subcontractus	Globata-Multiplicata	167.6	V	Côte d'Or-Vanvey	S	19.7	35
Asteracanthus	D103-p[b]	T-e	M. Bathonian	-	-	-	Gl	Gloucester (UK)	S	19.8	35
Asteracanthus	AST 54[b]	T-e	M.-L. Bathonian	Hodsoni-Subcontractus	Concinna-Multiplicata	166.8	Na	Ain-Nantua	LO	19.6	33
Notidanus	93365N[b]	T-e	M.-L. Bathonian	Hodsoni	Concinna	166.4	Tr	Isère-Trept	UOp	19.4	32
Pycnodont	93365P[b]	T-e	M.-L. Bathonian	Hodsoni	Concinna	166.4	Tr	Isère-Trept	UOp	19.4	39
Asteracanthus	P6-e[b]	T-e	M.-L. Bathonian	Hodsoni-Retrocostatum	Concinna-Digona	166.4-165.3	Au	Aisne-Aubenton	SPE	20.4	35
Mesodon	P1[b]	T-e	M.-L. Bathonian	Hodsoni-Retrocostatum	Concinna-Digona	166.4–165.3	Ra	Calvados-Ranville	UOPZ	21	45
Asteracanthus	P3-e[b]	T-e	M.-L. Bathonian	Hodsoni-Retrocostatum	Concinna-Digona	166.4–165.3	Ma	Sarthe-Mamers	S/UOPZ	19.9	42
Asteracanthus	P13[b]	T-e	M.-L. Bathonian	Hodsoni-Retrocostatum	Concinna-Digona	166.4–165.3	Mr	Pas-de-Calais-Marquise	S	20.6	37
Machimosaurus b.	92210	T-b	L. Bathonian	post-Hodsoni	post Concinna	<166.4	Ga	Indre-St Gaultier	P	19.4	40
Asteracanthus	93362[b]	T-e	L. Bathonian	post-Hodsoni	post Concinna	<166.4	Ga	Indre-St Gaultier	P	20.3	37
Asteracanthus	SERA-e[b]	T-e	L. Bathonian	Retrocostatum	Digona	165.3	Nu	Côte d'Or-Nuits St. Georges	protected	20.2	36
Asteracanthus	93360[b]	T-e	L. Bathonian	post-Retrocostatum	post-Digona	<165.3	W	Wiltshire (UK)	P (bay)	20.5	30
Asteracanthus	D71[b]	T-e	L. Bathonian	juste ante Discus	ante Eudesia	<164.6	Lq	Pas-de-Calais-Locquinghen	UOPZ	21.7	42
Asteracanthus	P12[b]	T-e	L. Bathonian	ante Discus	ante Eudesia	164.6	Mr	Pas-de-Calais-Marquise	UOPZ	22.3	40
Asteracanthus	Ja1[b]	T-e	L. Bathonian	Discus	Eudesia	164.6	Ja	Yonne-Jaulges	LO	20.3	40
Asteracanthus [c]	D21A[b]	T-e	L. Bathonian	Discus	Eudesia	164.6	LP	Côte d'Or-Les Perrières	LO	19.1	34
Pycnodont [c]	D19[b]	T-e	L. Bathonian	Discus	Eudesia	164.6	LP	Côte d'Or-Les Perrières	LO	18.8	35
Pycnodont [c]	D21P[b]	T-e	L. Bathonian	Discus	Eudesia	164.6	LP	Côte d'Or-Les Perrières	LO	18.7	34
Asteracanthus	D35[b]	T-e	L. Bathonian	Discus	Eudesia	164.6	Ri	Boulonnais-Rinxent	LO	21.3	37
Asteracanthus	Be-1A[b]	T-e	L. Bathonian	Discus-Bullatus	Eudesia-Divio	164.6–163.9	Me	Hte Saône-Merey	S	19.1	38
Asteracanthus	Bi[b]	T-e	E. Callovian	Bullatus	Divio	163.9	Bi	Yonne-Brion	S	20.2	35
Asteracanthus[c]	D25[b]	T-e	E. Callovian	Bullatus	Divio	163.9	D	Côte d'Or-Dijon	UOPZ	19.6	34
Asteracanthus	AST 55[b]	T-e	E. Callovian	Bullatus	Divio	163.9	La	Côte d'Or-Ladoix	UOPZ	19.0	36
Fish	D22	T-b	E. Callovian	Koenigi	Kalli	163.3	Ta	Côte d'Or-Talant	P	17.5	33
Asteracanthus	Be-2A[b]	T-e	E. Callovian	Koenigi	Kalli	163.3	Or	Doubs-Ornans	UOPZ	19.6	39
Crocodylian	D8	T-b	E. Callovian	Calloviense	Torqui	162.2	E	Côte d'Or-Etrochey	UOPZ	16.6	34
Pycnodus [c]	D11a[b]	T-e	E. Callovian	Calloviense	Torqui	162.2	E	Côte d'Or-Etrochey	UOPZ	20.0	37
Asteracanthus [c]	D10[b]	T-e	E. Callovian	Calloviense	Torqui	162.2	E	Côte d'Or-Etrochey	UOPZ	18.8	35
Metriorhynchus	N2	T-b	E. Callovian	Calloviense	Torqui	162.2	Ba	Calvados-Bavent	OBPZ	19.3	39

Table 1. (continued)

Vertebrate Taxa	Code	Sample	Stratigraphic Age	Ammonite Zones	Isochron	Age, Myr		Location	Depositional Environments	$\delta^{18}O$, ‰	P_2O_5, %
Asteracanthus	L6-e[b]	T-e	M. Callovian	Jason	Orbignyana	161.5	At	Hte Saone-Authoison	UOBPZ	19.1	37
Asteracanthus	M2[b]	T-e	M. Callovian	Coronatum	Oxoniensis	161.1	Pi	Vienne-Carrière des Lourdines	?	19.8	43
Notidanus	A1-L	T-b	M. Callovian	Coronatum	Oxoniensis	161.1	-	Wallücke (D)	LOBPZ	17.7	18
Asteracanthus	D37[b]	T-e	M. Callovian	Coronatum	Oxoniensis	161.1	E	Côte d'Or-Etrochey	UOBPZ	19.2	34
Asteracanthus	P2[b]	T-e	L.Callovian	Athleta	Athleta	160.3	Mi	Vendée-St. Michel en l'Herm	OBPZ	20.8	34
Asteracanthus	D36[b]	T-e	L.Callovian	Athleta	Athleta	160.3	Pr	Côte d'Or-Prusly s/ource	UOBPZ	18.9	39
Asteracanthus	D27[b]	T-e	L.Callovian	Athleta	Athleta	160.3	Ta	Côte d'Or-Talant	UOBPZ	19.5	30
Gyrodus	P5	T-b	L.Callovian	Athleta or Lamberti	Athleta or Lamberti	160.3–153.6	Mb	Sarthe-Marolles les Braults	UOBPZ	20.3	41
Sphenodus	93355	T-e	L.Callovian	Athleta or Lamberti	Athleta or Lamberti	160.3–153.6	Vo	Ardèche-La Voulte	UOdBZP	19.5	11
Marine reptile	93405	T-b	L.Callovian	Athleta or Lamberti	Athleta or Lamberti	160.3–153.6	Vi	Calvados-Vaches noires	UOBZP	21.7	38
Fish	N3	B	L.Callovian	Athleta or Lamberti	Athleta or Lamberti	160.3–153.6	Vi	Calvados-Villers-sur-mer	LOBPZ	20.3	27
Marine reptile	93404 R	T-b	L.Callovian	Lamberti	Lamberti	159.6	At	Hte Saône-Authoison	LOBPZ	18.7	28
Odontaspis l.	L41-e[b]	T-e	L.Callovian	Lamberti	Lamberti	159.6	At	Hte Saône-Authoison	LOBPZ	20.7	44
Notidanus m.	L126-b	T-b	L.Callovian	Lamberti	Lamberti	159.6	At	Hte Saône-Authoison	LOBPZ	19.4	42
Asteracanthus	W46[b]	T-e	L.Call-E. Oxf.	-	-	159.4	Vd	Vaud-Villeneuve	?	20.5	36
Asteracanthus	D39[b]	T-e	E. Oxfordian	Mariae	Mariae	159.1	-	Woodham (UK)	?	19.1	43
Notidanus m.	L5-b	T-b	E. Oxfordian	Cordatum-Mariae	Cordatum-Mariae	158.8	Ty	Jura-La Billode	O	18.4	16
Asteracanthus	Be-3A[b]	T-e	E. Oxfordian	Cordatum-Mariae	Cordatum-Mariae	158.8	Or	Doubs-Ornans	O	20.9	42
Asteracanthus	P11[b]	T-e	E. Oxfordian	Cordatum	Cordatum	158.5	To	Calvados-Trouville s/mer	UOBPZ	20.6	22
Asteracanthus	L3[b]	T-e	E. Oxfordian	Cordatum	Cordatum	158.5	Ty	Jura-Pont du diable	O	20.4	34
Lamnidae	B5L-e[b]	T-e	E. Oxfordian	Cordatum	Cordatum	158.5	Üe	Jura suisse-Üken (CH)	LOBPZ	21.5	33
Notidanus m.	93402-N-e[b]	T-e	E. Oxfordian	Cordatum	Cordatum	158.5	Ty	Doubs-Tarcenay	O	20.7	44
Odontaspis l.	93402-O[b]	T-e	E. Oxfordian	Cordatum	Cordatum	158.5	Ty	Doubs-Tarcenay	O	19.4	28
Reptile	D32	T-b	E. Oxfordian	Cordatum	Cordatum	158.5	Ar	Jura-Arcs/Montenot	O	18.7	34
Notidanus s.	W22-b	T-b	E. Oxfordian	Cordatum	Cordatum	158.5	Mf	Jura-Montfaucon (CH)	O	20.3	20
Pycnodus	P15p[b]	T-e	M. Oxfordian	-	-	-	Gn	Côte d'Or-Gigny	OBPZ	20.9	37
Reptile	P15R-e	T-e	M. Oxfordian	-	-	-	Gn	Côte d'Or-Gigny	OBPZ	19.3	40
Marine reptile	L14	T-b	M. Oxfordian	Plicatilis	Plicatilis	157.8	F	Hte Marne-Foug	UO(PZ)	20.8	32
Sphenodus sp.	R1[b]	T-e	M. Oxfordian	Plicatilis-Antecedens	Plicatilis-Transversarium	157.8–157.6	Vo	Ardèche-Ravin du Cheynier	UOdBZP	20.8	45
Pycnodont	D100-p[b]	T-e	M. Oxfordian	Plicatilis-Transversarium	Plicatilis-Transversarium	157.8–157.6	-	Yorkshire-(UK)	S	20.5	40
Pycnodontidae	B3p[b]	T-e	M. Oxfordian	Transversarium	Transversarium	157.6	U	Jura-St Ursanne (CH)	UOPZ	21.4	37
Sphenodus l.	93398-e[b]	T-e	M. Oxfordian	Transversarium	Transversarium	157.2	Cr	Ardèche-Crussol	UOdBZP	21	36
Sphaerodus sp.	D70[b]	T-e	M. Oxfordian	Transversarium	Transversarium	156.6	Ta	Côte d'Or-Talant	LOBPZ	21.5	45
Lamniform	B4L-e[b]	T-e	M. Oxfordian	Transversarium	Transversarium	156.9	Si	Jura-Siblingen (CH)	UOBPZ	21.1	27
Pycnodont	D106-p[b]	T-e	M.-L. Oxfordian	Transversarium-Bifurcatus	Transversarium-Bifurcatus	156.9–155.9	Vn	Meuse-Verdun	P	21.2	42
Pycnodus	P16[b]	T-e	L. Oxfordian	Bifurcatus	Bifurcatus	155.9	Ml	Yonne-Mailly le Chateau	UOPZ/S	20.6	40
Sphenodus l.	L1-d	T-b	L. Oxfordian	Bifurcatus	Bifurcatus	155.9	Ch	Jura-Chatelneuf	OBPZ	18	34
Sphenodus l.	L1-e[b]	T-e	L. Oxfordian	Bifurcatus	Bifurcatus	155.9	Ch	Jura-Chatelneuf	OBPZ	20.8	37
Sphenodus l.	L8-d	T-b	L. Oxfordian	Bifurcatus	Bifurcatus	155.9	Sa	Jura-Savigna	OBPZ	18.9	33
Sphenodus l.	L8-e[b]	T-e	L. Oxfordian	Bifurcatus	Bifurcatus	155.9	Sa	Jura-Savigna	OBPZ	20.6	37
Pycnodont [c]	L13[b]	T-e	L. Oxfordian	Bifurcatus	Bifurcatus	155.9	P	Meurthe et Moselle-Pagny	P	20.6	34
Asteracanthus	93363[b]	T-e	L. Oxfordian	Bifurcatus	Bifurcatus	155.9	He	Calvados-Hennequeville	UO	18.5	31

Table 1. (continued)

Vertebrate Taxa	Code	Sample	Stratigraphic Age	Ammonite Zones	Isochron	Age, Myr		Location	Depositional Environments	$\delta^{18}O$, ‰	P_2O_5, %
Pycnodont	B1p-e[b]	T-e	L. Oxfordian	Bimammatum	Bimammatum	155.2	Gä	Jura-Gächlingen (CH)	UOBPZ	20.5	38
Asteracanthus [c]	93364[b]	T-e	L. Oxfordian	Planula	Planula	154.4	T	Yonne-Tonnerre	UOZP	19.7	36
Teleosaurides	92154	T-b	L. Oxfordian	Planula	Planula	154.4	T	Yonne-Tonnerre	UOZP	16.5	33
Microdon	D108-p[b]	T-e	L. Oxfordian	Planula	Planula	154.4	T	Yonne-Tonnerre	UOpPZ	20	47
Asteracanthus	P19[b]	T-e	L. Oxf.to E. Kim.	Planula to Cymodoce	Planula to Cymodoce	155.2–152.3	Mc	Saône & Loire-Flacé Macon	P/UOPZ	19.7	42
Peloneustes	W19	T-b	E. Kimmeridgian	-	-	154.1–152.6	Ha	Seine maritime-Le Havre	O	20.7	34
Sphaerodus sp.	W29	T-e	E. to L. Kimmeridgian	-	-	-	Ne	Jura-La Neuveville (CH)	P/UOPZ	22	41
Pycnodont	D69	T-e	Kimmeridgian	-	-	-	Gr	Hte Saône-Arc-les Gray	?	21.3	44
Pycnodont	D33[b]	T-e	L. Kimmeridgian	Mutabilis or Eudoxus	Mutabilis or Eudoxus	152.3–151.4	Do	Aube-Dolancourt	UOpPZ	20	39
Sphaerodus sp.	W26[b]	T-e	L. Kimmeridgian	-	-	152.6–150.7	Vd	Vaud-Ste Croix (CH)	UOpPZ	21.4	43
Pycnodont	D107-p[b]	T-e	E. Tithonian	Gigas	Gigas	150.2	Bo	Aube-Bourguignons	UOpPZ	20.8	41
Sphaerodus sp.	D45[b]	T-e	E. Tithonian	Gigas	Gigas	150.2	Mt	Haute Saône-Mantoche	UOpPZ	20.7	37
Mesodon gigas	D46[b]	T-e	E. Tithonian	Gigas	Gigas	150.2	Mt	Haute Saône-Mantoche	UOpPZ	20.1	42
Sphaerodus sp.	D68[b]	T-e	E. Tithonian	Gigas	Gravesiana	150.2	No	Haute Saône-Noiron	UOpPZ	20.4	43
Pycnodus	93396[b]	T-e	Portlandian	-	-	144.2–145.6	Sl	Soleure (CH)	?	20.0	44
Pycnodus gigas	Be5-p[b]	T-e	Portlandian	-	-	144.2–145.6	Cx	La Chaux de fonds (CH)	?	21.1	42
Mesodon gigas	93471	T-e	Portlandian	-	-	144.2–145.6	Vl	Doubs-Villers -le-lac	?	20.6	24

[a]Note that *Microdon*, *Mesodon*, *Pycnodus* genera are all Pycnodontidae. Stratigraphic ages for isochrons were reported on the ammonite biostratigraphic scale and on the absolute scale proposed by *Gradstein et al.* [1994]. P_2O_5 wt % of biogenic apatites were calculated considering a mean value of 80 ± 3% for the silver phosphate chemical yield obtained with NIST NBS120c. Depositional environments: P, protected; S, = shoreface; O, offshore; U, upper; L, lower; PZ, photic zone; BPZ, below photic zone; p, proximal; d, distal. Samples: B, bone; T, tooth; b, bulk; d, dentine; e, enamelloïd.

[b]Values used in Figure 5.

[c]Data that were previously published in the work of *Picard et al.* [1998].

constituting a condensed image of fauna and flora activity occurring from surface to bottom waters, also cannot provide information on living depths in the water column. Previous studies, however, indicate that pycnodont fish have been mostly marine, and only in some cases estuarine to freshwater dwellers [*Martill*, 1990; *Nursall*, 1996; *Poyato-Ariza et al.*, 1998]. Pycnodonts must have been an important component of tropical and subtropical coral reef communities, analogous to balistid fish in modern oceans [*Nursall*, 1996]. *Asteracanthus* sharks are considered as being essentially marine, but their ecology is poorly known [*Cappetta*, 1987]. Other sharks, with lamniform teeth, were probably piscivorous [*Cappetta*, 1987; *Martill*, 1990].

[11] Enamel is more resistant than dentine or bone to post-depositional oxygen isotope exchange [e.g., *Sharp et al.*, 2000] because of its high degree of mineralization, therefore this phosphatic tissue was preferentially selected and separated mechanically with a microdrill under a binocular (Table 1). In the case of the smallest teeth, a few bulk isotopic analyses were performed because it was not possible to separate enough enamel.

[12] Similarly, carbonate ions that are present in the apatite structure are supposed to be less resistant than phosphate ions to oxygen isotope exchange during diagenetic alteration [*Iacumin et al.*, 1996; *McArthur and Herczeg*, 1990]. To test the state of preservation of Jurassic teeth, we have measured the oxygen isotope compositions of both phosphate and carbonate in fifteen fish and six reptile teeth.

4. Analytical Methods

[13] Carbonate apatite samples were first treated with a 3% sodium hypochlorite solution for 4 hours to remove organic matter and rinsed three times with distilled water. Then they were treated with a 1M acetic acid-acetate buffer for two days to remove exogenous carbonates according to the method presented by *Bocherens et al.* [1996]. Oxygen and carbon isotope ratios from the carbonate in substitution in the apatite were determined using the phosphoric acid method [*McCrea*, 1950] with a reaction time of 48 hours at 30°C. Reproducibility for carbon and oxygen isotope measurements in carbonates were ±0.05‰ and ±0.1‰, respectively.

[14] Phosphate radicals were isolated from biogenic apatites as Ag_3PO_4 crystals using the method of *Crowson et al.* [1991] modified by *Lécuyer et al.* [1993]. Silver phosphate was reacted with graphite at 1100°C to produce pure CO_2 [*Lécuyer et al.*, 1998] (modified after *O'Neil et al.* [1994]). The quality of the reaction, marked by the absence of CO production, was monitored by the carbon isotope composition of CO_2 derived from the graphite (Figure 2a). Carbon dioxide was analyzed with a VG Prism™ mass spectrometer. All data are quoted in the δ notation relatively to SMOW, via calibration on NBS18 and NBS19 international standards. Several tooth enamels, including all those with extreme δ values were duplicated. Repeated analyses of the phosphorite NBS120c gave a mean $\delta^{18}O$ value of 21.68 ± 0.19‰ (Figure 2b). The CO_2 gave a mean $\delta^{13}C$ value of −23.51 ± 0.11‰ (Figure 2c), similar to that of graphite analyzed by the CuO method ($\delta^{13}C = -23.5 \pm 0.05$‰). The P_2O_5 contents of samples were calculated from their chem-

ical phosphate yields using the average yield of 80 ± 3% obtained for the NBS120c phosphorite that contains 33.33% of P_2O_5 (Table 1).

[15] Diagenetic alteration of fossil apatite was detected in eleven samples during the chemical procedures using the following criteria: (1) recovery of silver phosphate down to 60% (Table 1), because of the replacement of phosphates by carbonates, silica or metal oxides (samples A1-L, 93355, L5b, 93471), (2) solutions that turned from red to yellow during neutralization with KOH (O1, N3, D22, 93355, D28), revealing the presence of metal oxides (Fe, Mn, Al), and (3) both low $\delta^{18}O$ values of $PO4^{3-}$ and $\delta^{13}C$ values of graphite (Figure 2a) for samples L11, 92154, D8 and D28, indicating the presence of exotic organic molecules that were not totally eliminated during the wet chemical procedures [*Lécuyer*, 2003].

5. Results

[16] Oxygen isotope compositions of phosphate from Jurassic fish and reptiles are reported in Table 1. Analyses of associated dentine and enamel from two teeth of Chondrichtyan lamnidae (samples L8 and L1) gave chemical phosphate yields that are about 10% lower for the dentine than for the enamel. The dentine has $\delta^{18}O$ values from 1.7 to 2.8‰ lower than the enamel (Table 1), which indicates strong isotopic disequilibria between the two coexisting phosphatic tissues. Similar observations were made by *Sharp et al.* [2000] and *Puceat et al.* [2003]. Massive enamel of *Asteracanthus* and pycnodonts have high mean P_2O_5 percentages with relatively low variance (36.7 ± 3.6% and 39.3 ± 3.4%, respectively), bracketing those obtained on enamels from tearing teeth (38.2 ± 6.8%; n = 13) that have a microstructure close to that of modern lamnidae. By contrast, bulk fish teeth and bones have variable and low P_2O_5 contents (31.6 ± 6.9%) and constitute a fossil material that commonly suffered chemical and isotopic alterations.

[17] The range and mean $\delta^{18}O$ values of all well-preserved vertebrate taxa (where no indicators of diagenesis were observed) are reported in Table 2. Similar ranges and mean $\delta^{18}O$ values were obtained with *Asteracanthus* and Pycnodontidae enamels from the Bathonian-Callovian (19.5 ± 0.5 and 19.6 ± 0.7‰) and Oxfordian-Tithonian (20.1 ± 0.6 and 20.7 ± 0.5‰) periods. Mean $\delta^{18}O$ values for other vertebrates like *Notidanus* (20 ± 0.7‰) and *Odontaspis* (20 ± 0.7‰) sharks, though based on a very limited number of samples, have similar values to those documented for *Asteracanthus* and Pycnodontidae. Mean $\delta^{18}O$ values for Chondrichtyan *Sphenodus* (20.8 ± 0.2‰) and Osteichtyan *Sphaerodus* (21.2 ± 0.6‰) are higher than those for *Asteracanthus* and Pycnodontidae *sensu stricto*, but they are mainly restricted to the Late Jurassic, a period characterized by higher $\delta^{18}O$ values than those documented throughout the Middle Jurassic. The more positive $\delta^{18}O$ values for *Sphenodus* and *Sphaerodus* may indicate that they lived in deeper waters and do not record surface temperatures unlike *Asteracanthus* seems to do (Figure 3). However, we note that Pycnodontidae have $\delta^{18}O$ values indistinguishable from those of *Asteracanthus* during the Bathonian-Callovian and they constitute the most abundant fossil fauna analyzed during the Oxfordian-Tithonian period (Table 2). Therefore the high $\delta^{18}O$ values of Oxfordian fish teeth can be considered as also recording the temperature of the upper part of the water column.

[18] Mean $\delta^{18}O$ values of middle Bathonian to late Callovian (168–160 Myr) *Asteracanthus* have been calculated for the various depositional paleoenvironments documented in the eastern part of the Basin (Figure 3). Note the uniformity of the $\delta^{18}O$ values of *Asteracanthus* teeth (from 19.2 ± 0.2 to 19.7 ± 0.6‰) that are preserved in inner to outer depositional environments. Middle to late Bathonian samples from the western and northwestern part of the basin (Boulonnais, Normandy, and Poitou regions) have $\delta^{18}O$ values that are on average 1.5‰ higher than their southeastern counterparts (Table 1). Samples from the central region (Ja1, Bi, SERA, Table 1) have intermediate oxygen isotope ratios, confirming the existence of an isotopic gradient across the whole basin.

[19] The Bajocian to the Tithonian fish tooth samples from the eastern part of the basin show $\delta^{18}O$ variations over 20 Myr (Figure 4). These isotopic variations define an envelope from 0.5 to 1.5‰ wide for the various isochrons. This isotopic range is comparable to the one measured by *Vennemann et al.* [2001] on recent fish teeth, which is typically between 0.6 and 1.1‰ for different teeth from a single shark. This naturally occurring variation in oxygen isotope compositions recorded in fish teeth may reflect the diversity of the living environments which includes: (1) thermal gradients within the water column; (2) seasonal thermal variations since the growth of a fish tooth represents less than a year (several weeks to several months depending on species), but they should remain limited under tropical latitudes; (3) coastline proximity and the influence of freshwater inputs; and (4) the possible occurrence of surficial oceanic currents.

[20] Three major stages may be distinguished: (1) a period of decreasing $\delta^{18}O$ values from 20 to 19‰ for the Bajocian to Bathonian interval, (2) a rapid increase of $\delta^{18}O$ values up to 21‰ initiated during the late Callovian and reaching a maximum during the early-middle Oxfordian, and (3) another stage of decreasing $\delta^{18}O$ values, similar in amplitude to stage 1, starting in the late Oxfordian to reach values of 20‰ around the Oxfordian-Kimmeridgian boundary.

[21] Oxygen isotope compositions of carbonates from Jurassic fish teeth range from 24.5 to 30.0‰ whilst those of reptiles range from 23.6 to 30.4‰ (Table 3). For fish teeth, differences between the $\delta^{18}O$ values measured in apatite carbonate and its associated phosphate oxygen (Δc-p) range from 7.0 to 9.5‰, except for two samples; a whole tooth (L12; Δc-p = 5.0‰) and one altered sample (93355; Δc-p = 5.7‰). These values are within or close to the known fractionations (Figure 5) between apatite carbonate and phosphate oxygen [*Longinelli and Nuti*, 1973; *O'Neil et al.*, 1969; *Iacumin et al.*, 1996].

[22] The amount of carbonate substituted in the apatite structure of Jurassic fish tooth enamel ranges from 3.9 to 5%, except for samples D21P and 93357 (Table 3). These values match those of 4–5% that were measured in present-

A)

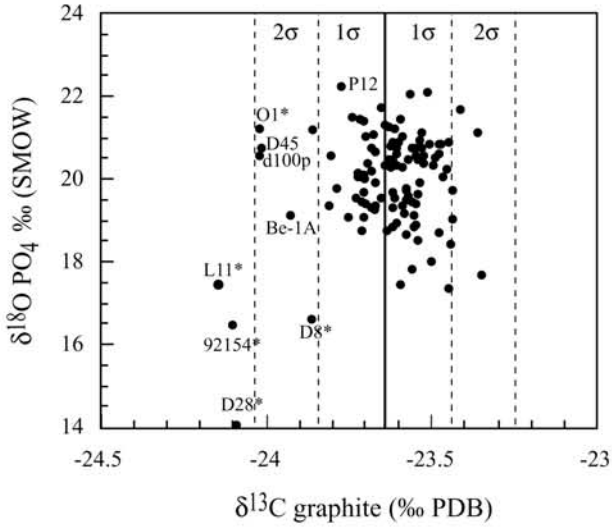
2σ
1σ
1σ
2σ
P12
O1*
D45
d100p
Be-1A
L11*
92154*
D8*
D28*
24
22
20
18
16
14
-24.5
-24
-23.5
-23
δ18O PO4 ‰ (SMOW)
δ13C graphite (‰ PDB)

B)

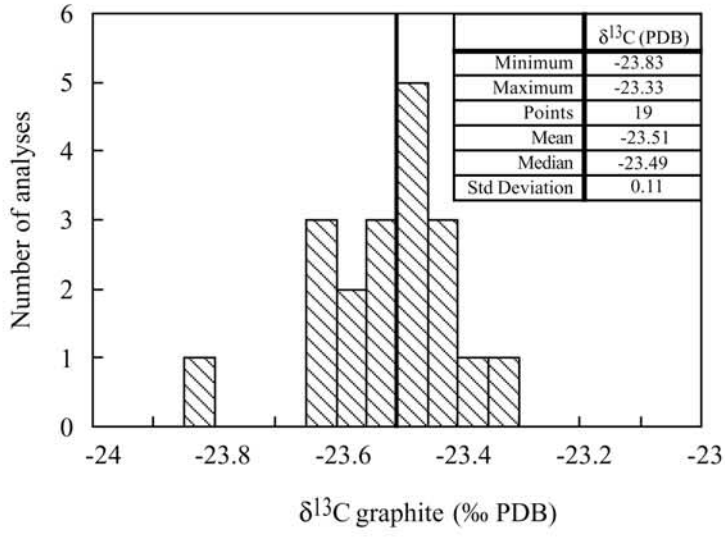
δ13C (PDB)
Minimum -23.83
Maximum -23.33
Points 19
Mean -23.51
Median -23.49
Std Deviation 0.11
Number of analyses
6
5
4
3
2
1
0
-24
-23.8
-23.6
-23.4
-23.2
-23
δ13C graphite (‰ PDB)

C)

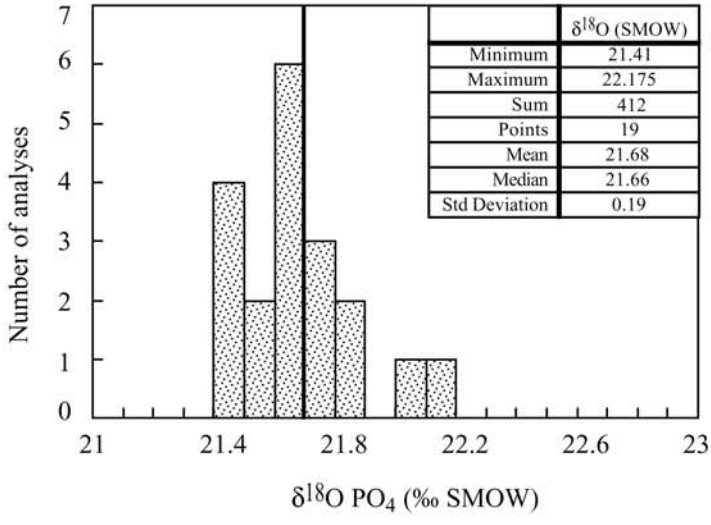
δ18O (SMOW)
Minimum 21.41
Maximum 22.175
Sum 412
Points 19
Mean 21.68
Median 21.66
Std Deviation 0.19
Number of analyses
7
6
5
4
3
2
1
0
21
21.4
21.8
22.2
22.6
23
δ18O PO4 (‰ SMOW)

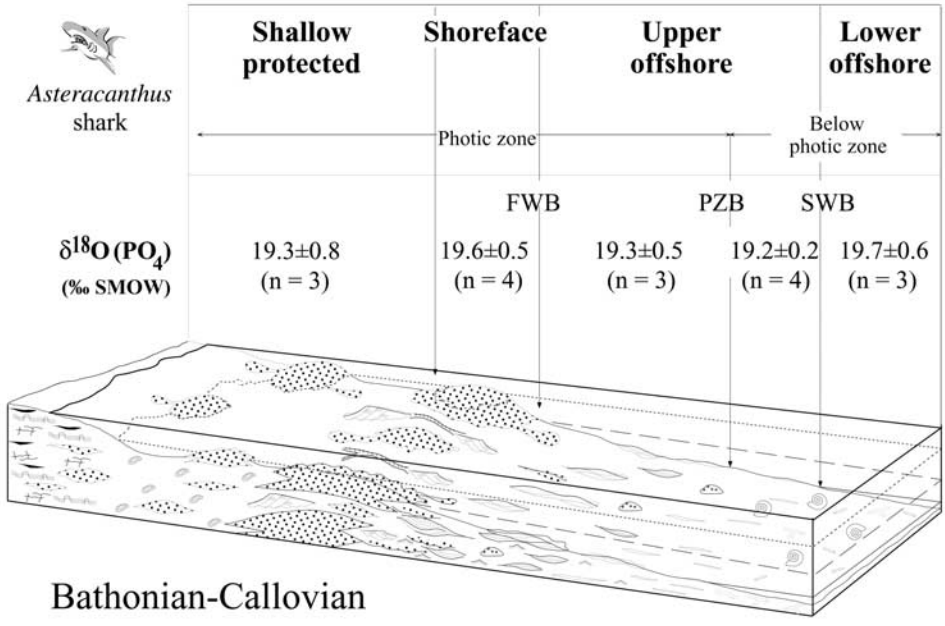

Figure 3. Mean $\delta^{18}O$ values calculated for the studied collection of *Asteracanthus* sharks through the Bathonian-Callovian interval. Oxygen isotope compositions are reported along a general depositional environment profile (modified from *Gaumet et al.* [1996]). Environments were defined by hydrodynamic limits that are the fair weather base (FWB), the storm wave base (SWB), and by the occurrence of photosynthetic organisms (PZB = base of the photic zone). Note the relative constancy within uncertainties of sharks' $\delta^{18}O$ values with deepening of the basin, thus indicating that they record sea surface temperatures.

day vertebrate teeth [*LeGeros and LeGeros*, 1984; *Michel et al.*, 1995]. The bulk tooth L12 has a low CO_3^{2-} content of 2.9‰ and a low Δc-p of +5 both diagnostics of a diagenetic alteration of the carbonate component of the apatite. The reptile bulk teeth have CO_3^{2-} contents that range from 3.8 to 7%.

6. Discussion

6.1. Diagenetic Perturbations

[23] We conclude from our observations during the chemical procedures that seven vertebrate whole teeth (i.e., <8% of the enamel samples) and the two fish bone fragments have been chemically and isotopically modified by diagenetic processes. Only one enamel from a *Sphenodus* tooth (93355) and one enamel from a massive tooth (93471) are suspect on the basis of the selected criteria. Some of these phosphate samples are depleted in ^{18}O relative to coexisting or associated enamel (D28; D22; A1-L; Table 1). Moreover, only two fish teeth (enamel 93355 and whole tooth L12) plot outside the domain of apparent oxygen isotopic equilibrium between phosphate and carbonate, limited by previously proposed fractionation equations (Figure 5). This suggests that most enamels from Jurassic teeth have conserved their primary isotopic signatures.

[24] On the basis of oxygen isotope analyses of modern teeth, dentines are depleted in ^{18}O by up to 1.7‰ relative to associated enamel [*Vennemann et al.*, 2001]. For comparison, Jurassic dentines from two lamniform teeth show $\delta^{18}O$ values up to 2.8‰ lower than coexisting enamel, suggesting that these dentines have been significantly altered. Consequently, we do not consider bulk samples for paleoenvironmental studies even if some of them have $\delta^{18}O$ values in the range of contemporaneous fish enamel (W22-b, L126-b, L12; Table 1). The greater resistance of Jurassic enamels to diagenetic processes than either dentine or bone supports

Figure 2. (opposite) Stable isotope compositions of CO_2 from Ag_3PO_4 of Jurassic apatites and phosphorite standard NBS120c. (a) $\delta^{13}C$ and $\delta^{18}O$ values of CO_2 from Ag_3PO_4 of Jurassic apatites after reaction with graphite at 1100°C. Note that most samples having $\delta^{13}C$ values close to the lower limit of the envelope (defined with 2σ a 95% of confidence level) were diagenetically altered (*), except D45, d100p, and Be-1A (see text for more explanations). (b and c) Frequency histograms of carbon and oxygen isotope compositions of CO_2 from repeated analyses of the phosphorite NBS120c after reaction of silver phosphate with graphite at 1100°C. The small standard deviations for O and C, of 0.19‰ and 0.11‰ respectively, indicate that oxygen from silver phosphate was converted into CO_2 without significant production of CO [*Lécuyer*, 2003].

Table 2. Statistics of Mean $\delta^{18}O$ Values Calculated for Dental Apatite From *Asteracanthus*, *Pycnodont*, and *Sphenodus* for the Bathonian-Callovian and Oxfordian-Tithonian Ontervals

Period/Fauna	*Asteracanthus*, n = 19	*Pycnodont*, n = 7	*Sphenodus*, n = 1
	Bathonian-Callovian		
Mean	19.48	19.57	19.50
Standard deviation	0.51	0.65	0.00
Minimum	18.70	18.70	19.50
Maximum	20.30	20.50	19.50
	Asteracanthus, n = 7	*Pycnodont*, n = 11	*Sphenodus*, n = 4
	Oxfordian-Tithonian		
Mean	20.13	20.71	20.80
Standard deviation	0.64	0.47	0.16
Minimum	19.10	20.00	20.60
Maximum	20.90	21.40	21.00

earlier studies realized on Mesozoic vertebrate teeth [*Kolodny et al.*, 1996; *Sharp et al.*, 2000].

6.2. Vertebrate $\delta^{18}O$ Values and Sea Surface Temperatures

[25] Oxygen isotope analysis of apatite from modern selachians has shown that isotopic temperatures reflect the average temperature of the seawater layer in which the fish lives [*Picard et al.*, 1998]. Although the living depths of Jurassic vertebrate taxa are not known, estimates can be made. Marine bottom temperatures can be derived from the $\delta^{18}O$ values of brachiopods giving a lower limit for the water column [*Picard et al.*, 1998]. Isotopic temperatures inferred from the $\delta^{18}O$ values of brachiopods sampled from known different depositional environments can be compared with the temperatures derived from the associated vertebrate $\delta^{18}O$ values. Note that if the vertebrates and brachiopods were living at the same time and place (associated fossils), they were not necessarily present in the same water layer.

[26] Mean $\delta^{18}O$ values, calculated for both middle Bathonian to late Callovian *Asteracanthus* sharks from the eastern part of the Anglo-Paris basin, are reported in Figure 3 as a function of their depositional environment. The isotopic values, ranging from 19.2 ± 0.2 to 19.7 ± 0.6‰, remain relatively constant independent of the deepening of the marine basin from the shoreface to lower offshore environments at about 200 m depth. This pattern of isotopic distribution strongly contrasts with the $\delta^{18}O$ values of coexisting brachiopods that increase with depth and record thermal differences of up to 12°C between surface and lower offshore bottom waters [*Picard et al.*, 1998]. These observations suggest that the oxygen isotope compositions of *Asteracanthus* sharks record temperatures close to sea surface temperatures.

[27] Isotopic temperatures are calculated from the fractionation equation determined by *Kolodny et al.* [1983] on the basis of various fresh and seawater fish species. A similar equation (Figure 6) is deduced from present-day

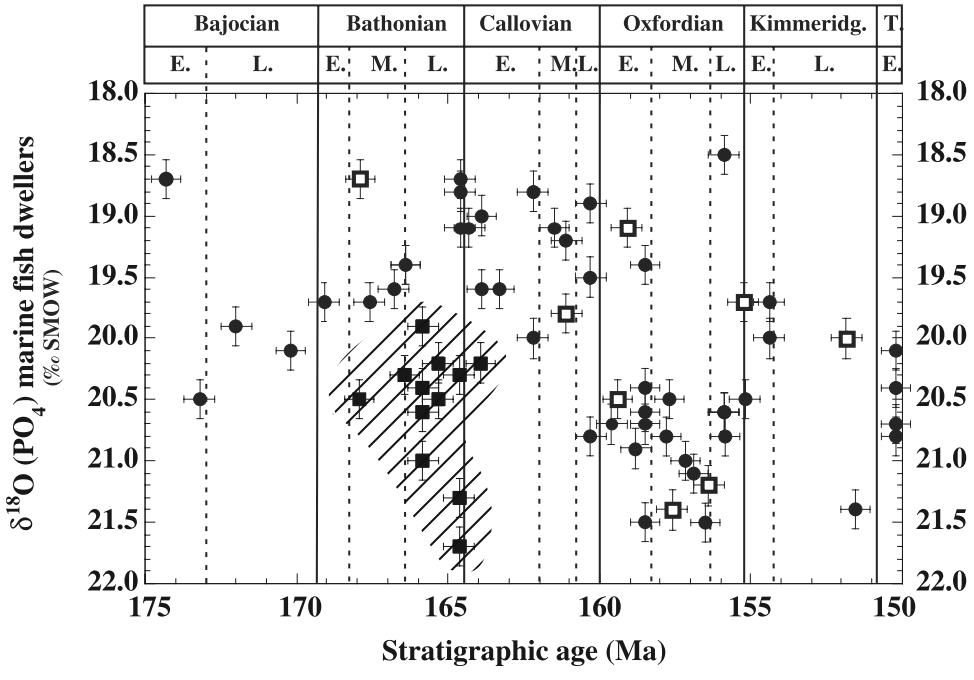

Figure 4. Variations of $\delta^{18}O$ values of fish tooth enamel from the Bajocian-Tithonian of the Anglo-Paris basin. Fish teeth were sampled on isochrons with an approximate resolution of 1 Myr. During the Bathonian, fish samples from the northwestern part of the Anglo-Paris basin define a colder water mass (dashed area) in comparison to contemporaneous samples from the southern eastern part. The appearance of boreal ammonites *Cardioceratidae* during the late Callovian-middle Oxfordian is synchronous with an increase in fish tooth $\delta^{18}O$ values. Open squares indicate fish samples coming from protected and poorly controlled environments.

Table 3. Oxygen Isotope Compositions and Mass Fractions of Structural Carbonate From a Selection of Fish and Reptile Apatites

Sample Code	$\delta^{18}O(CO_3)$	$\Delta(CO_3\text{-}PO_4)$	CO_3, wt %
	Fish		
L13 (T-e)	29.1	8.5	nd[a]
93364 (T-e)	27.6	7.9	5.2
93355 (T-e)	25.2	5.7	n.d.
D27 (T-e)	28.4	8.9	n.d.
D10 (T-e)	26.7	7.9	n.d.
D25 (T-e)	26.6	7.0	4.7
D11a (T-e)	27.2	7.2	3.9
93362 (T-e)	28.6	8.3	4.8
D21A (T-e)	27.7	8.6	5.4
D21P (T-e)	26.7	8.0	8.0
93357 (T-e)	28.2	7.7	7.5
D6 (T-e)	27.9	8.2	5.1
93360 (T-e)	30.0	9.5	4.5
L10 (T-e)	28.0	7.9	5.5
L12 (T-b)	24.5	5.0	2.9
	Reptiles		
92154 (T-b)	23.6	7.1	3.8
93405 (T-b)	30.4	8.7	4.4
D8 (T-b)	25.3	8.7	n.d.
92210 (T-b)	27.4	8.0	4.2
93369 (T-b)	27.3	6.5	7.0
L11 (T-b)	26.0	8.5	4.4

[a]Nd, not determined.

shark and water isotopic data published in the work of *Picard et al.* [1998].

[28] Assuming a $\delta^{18}O$ value of 0‰ compatible with both the absence of continental ice caps and the high-salinity of low-latitude surface sea waters, isotopic temperatures of 27 to 29°C are calculated, and are comparable to surface temperatures measured in modern tropical platform waters [*Adlis et al.*, 1988]. Similar $\delta^{18}O$ values, and therefore isotopic temperatures, of contemporaneous sharks (*Asteracanthus*, *Notidanus, Odontaspis* and *Sphenodus*) and Pycnodontidae (Tables 1 and 2) strongly suggest that these fish were principally restricted to surface waters. They are used to reconstitute sea surface temperatures.

6.3. Basin-Scale Oxygen Isotope Variations

[29] Three different interpretations may be formulated to explain the $\delta^{18}O$ spread of 3‰ identified throughout the Anglo-Paris basin from the Middle to Late Jurassic. In terms of salinity changes, it would correspond to variations of up to 7.5 ppt over the basin, assuming a 2.5 ppt salinity increase for 1‰ increase of $\delta^{18}O$ value of seawater under subtropical latitudes [*Craig and Gordon*, 1965]. Such salinity gradients seem unrealistically large without any known physical barrier isolating the western part of the basin from the east.

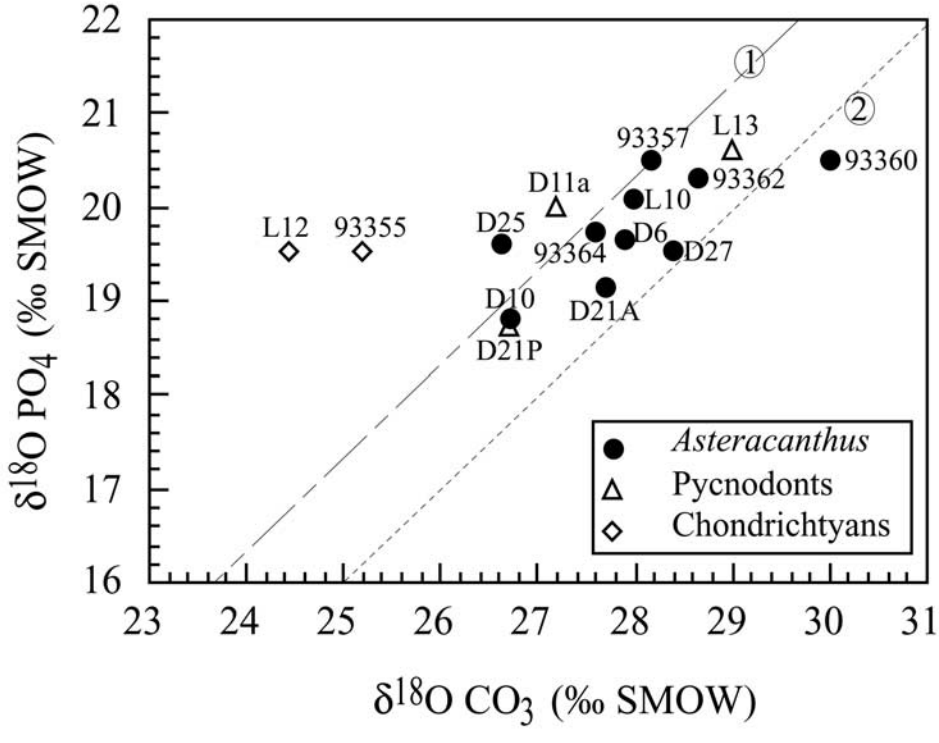

Figure 5. $\delta^{18}O$ measurements of phosphate tooth enamel and structural carbonate from Jurassic fish apatites of the Anglo-Paris Basin. Previously proposed fractionation equations between phosphate and carbonate are also reported: 1, *Longinelli and Nuti* [1973] and *O'Neil et al.* [1969]; 2, *Iacumin et al.* [1996]. Except for two undetermined chondrichtyan teeth, Jurassic *Asteracanthus* and pycnodontidae fall between the two curves of oxygen isotope fractionation.

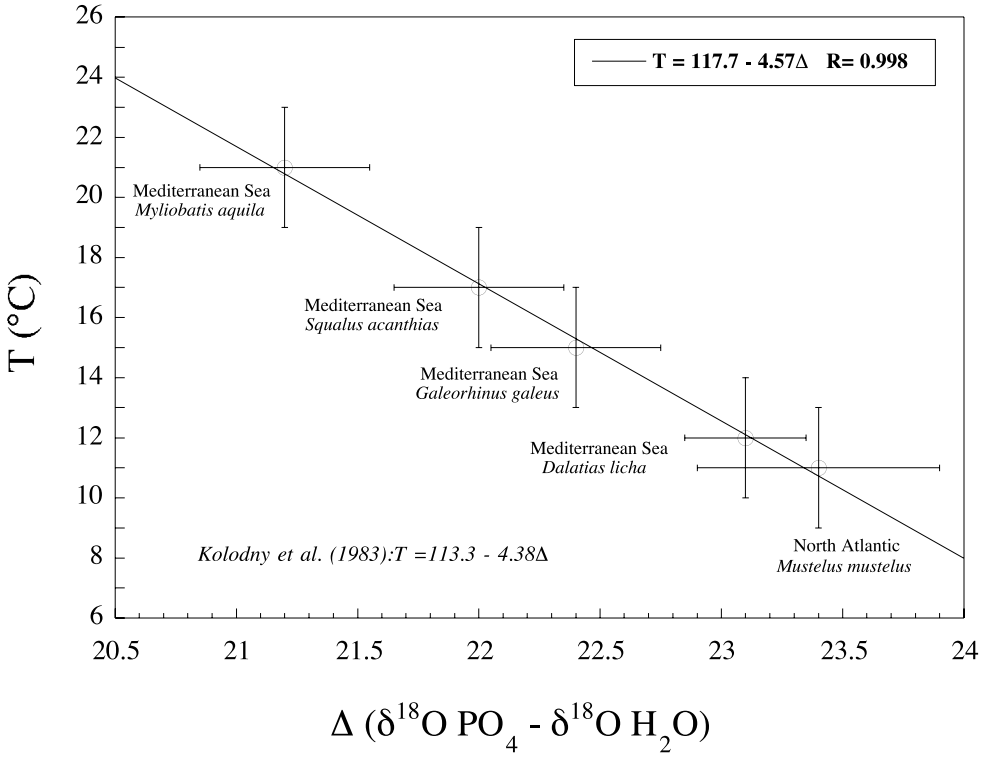

Figure 6. Oxygen isotope fractionation between present-day shark phosphate and ambient seawater. Data come from *Picard et al.* [1998]. Note that this equation is comparable to the equation published by *Kolodny et al.* [1983], which was determined by using modern fresh and sea water fish species.

Additionally, no evidence for excessive evaporation over precipitation is provided by the sedimentary record in the western domain of the Anglo-Paris basin. The highest $\delta^{18}O$ fish values are observed in the Boulonnais (Samples D35, D71, P12; Table 1; Figures 1 and 4) where estimated water depths are 50–200 m for the upper to lower offshore deposits [*Vidier et al.*, 1995; *Garcia et al.*, 1996].

[30] An apparent variation in the isotopic temperatures of 15°C is observed over a 3° change of paleolatitudes between the Boulonnais and the Burgundy platform (Figures 4 and 7). Such a thermal gradient of 5°C/°Lat. is unrealistically too high when compared to modern thermal gradients that are generally lower than 1°C/°Lat [*Savin*, 1977] (see also http://ingrid.ldeo.columbia.edu)

[31] For the middle-late Bathonian, we observe that the $\delta^{18}O$ fish values progressively decrease along a north-south direction (Figure 7). This distribution may be due to the influx of a cool current that progressively becomes warmer southward. This water mass of boreal origin probably had a $\delta^{18}O$ value lower than that more typical of tropical waters, taken here to be 0‰, consequently, calculated temperatures must be considered as maximal values. During the late Bathonian, isotopic temperatures may have been close to (1) 19°C in the northern part of the basin, in the Boulonnais and Normandy, (2) 24°C in the central part and, (3) 28–31°C in the southeast. Such temperature gradients of 10°C over a few hundred kilometers have modern analogues such as the area between the east U.S. coast and Bermuda where the Gulf Stream heads northeast from the Sargasso Sea [*Brown et al.*, 1989]. The proposed cool current may have resulted from the opening of the North Sea rift that was initiated during the middle-late Bathonian [*Ziegler*, 1988]. Cool waters, formed at high paleolatitudes in the Boreal Arctic domain, could have flowed southward to mix progressively with the western Tethys. The connection between the basins was probably limited during the middle Bathonian; during this period, corridors were filled with protected sandy environments and deltaic shales, both characterizing water depths less than 30 m [*Ziegler*, 1988]. The late-Bathonian Eudesia isochron corresponds to the most extensive flooded surface and coincides with the first brief excursion of boreal ammonites into the Anglo-Paris Basin [*Marchand and Thierry*, 1974, 1997; *Cariou et al.*, 1985], confirming a real communication between the Tethyan and Boreal basins and the influx of cold waters.

6.4. Middle-Late Jurassic Evolution of Tropical SST in the Anglo-Paris Basin

[32] At tropical latitudes, the evaporation/precipitation ratio tends to be higher than 1 resulting in increased salinity and $\delta^{18}O$ values of surface waters relative to mean ocean water. ^{18}O-enrichment of about 1‰ relative to SMOW has been documented for present-day tropical surface waters [e.g., *Craig and Gordon*, 1965; *Carpenter and Lohmann*, 1995; *Gonzalez and Lohmann*, 1985]. Therefore isotopic temperatures of surface waters have been derived from the $\delta^{18}O$ record of biogenic phosphates through the Middle-Late Jurassic (≈20 Myr), assuming a $\delta^{18}O$ seawater of 0‰. This hypothesis has been retained considering both the tropical paleolatitudes of western Europe and the absence

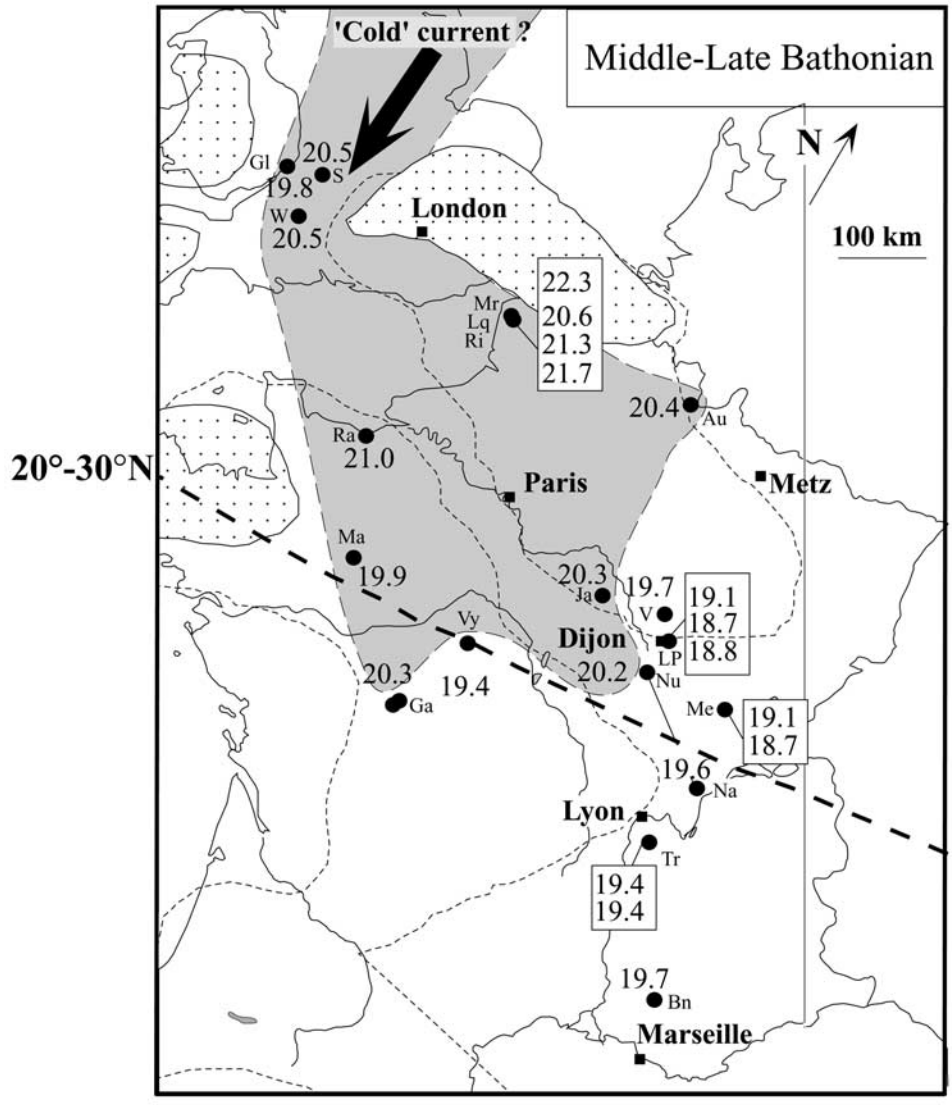

Figure 7. Geographical map of the Anglo-Paris Basin with the regional distribution of fish tooth $\delta^{18}O$ values for the middle-late Bathonian. The gray area encloses isotopic compositions higher than 20‰. This regional distribution of $\delta^{18}O$ values could have resulted from the presence of a cold oceanic current originating from boreal realms.

of polar ice caps as a first approximation. Sea surface temperatures (SST) inferred from surface dwellers (*Asteracanthus* and Pycnodontidae) increased from 25°C to 30°C on average over ≈7 Myr from late Bajocian to late Bathonian then decreased down to 20°C in the middle Oxfordian boundary in ≈8 Myr (Figure 8). This thermal minimum is followed by a warming of 5°C of surface waters during the late Oxfordian and early Kimmeridgian.

[33] The apparent cooling of surface waters that was initiated during the late Callovian Lamberti zone and that attained a maximum during the early-middle Oxfordian relates with the colonization of the western Tethys by the boreal ammonites of the Cardioceratidae family [*Marchand and Thierry*, 1974, 1997; *Cariou et al.*, 1985]. Such a cooling episode may have corresponded to the southward propagation of a boreal oceanic current and/or to a global climate change. There is no available evidence for the existence of a cold oceanic current throughout the major part of the Oxfordian. Studies of the distribution of the wood genus *Xenoxylon* and palynomorphs argue for a temperate and wet climate during the early Oxfordian in western Europe [*Philippe and Thévenard*, 1996; *Abbink et al.*, 2001]. All these data support the existence of a cooling episode that affected both marine and terrestrial environments of the western Tethyan domain.

[34] Perturbations of the carbon cycle due to volcanism or changes in the rates of burying organic matter could have induced temperature oscillations at the timescale of a few million years. According to *Dromart et al.* [1996], the warm Bathonian-Callovian phase could be related to large CO_2 fluxes released by contemporaneous arc-related volcanism in Patagonia at 164.1 Myr [*Féraud et al.*, 1999] and South

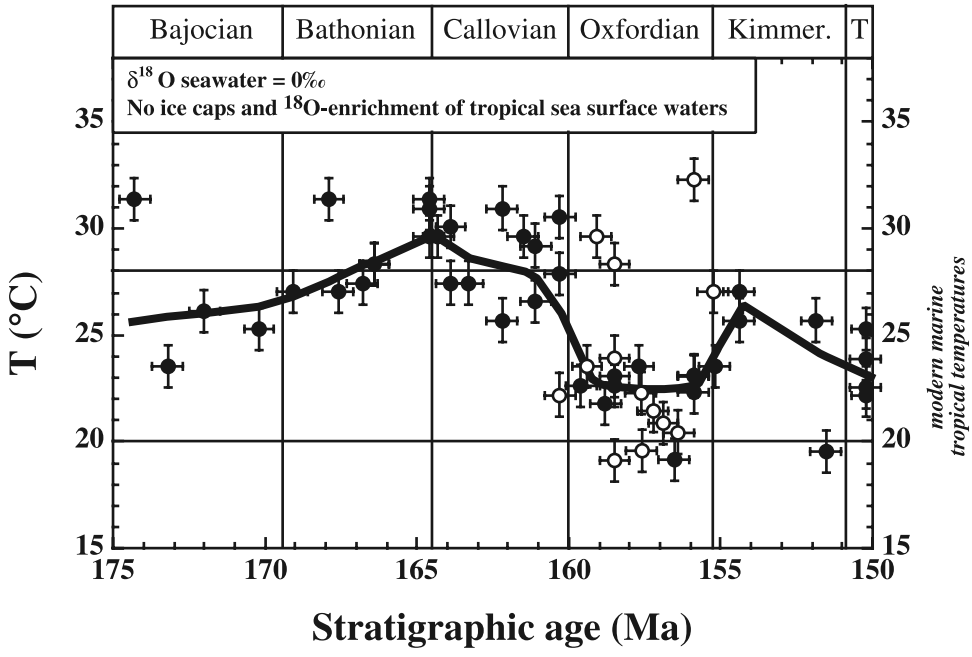

Figure 8. Evolution of isotopic temperatures calculated with a $\delta^{18}O$ of seawater = 0‰, from the Bajocian to the Tithonian. The area between the two horizontal plain lines covers the present-day range of sea surface tropical temperatures. The fitting curve was obtained by using only the *Asteracanthus* and Pycnodont assemblages (filled circles) from the eastern part of the basin using a least square method with 20% weight. Open circles indicate tearing sharks.

China at 164.6 Myr [*Davis et al.*, 1997]. Organic rich-layers deposited during the middle Callovian could have sequestered carbon and lowered atmospheric CO_2 levels, thus initiating the global cooling stage at the Callovian-Oxfordian boundary.

[35] With the hypothesis of a constant isotopic composition of seawater of 0‰, we calculated tropical surface temperatures ranging from 25°C to 30°C for the eastern basin during the Bajocian throughout the Callovian. This temperature range is slightly higher than modern thermal variations (19°C to 27°C) measured in shallow waters (≈50 m) under similar latitudes (20–30°) in analogous carbonate platforms [*Adlis et al.*, 1988] (Ocean Atlas data, Scripps Institute of Oceanography). By contrast, middle Oxfordian isotopic temperatures of 20°C are rather low considering the presence of coral reefs in the Swiss Jura [e.g., *Gygi and Persoz*, 1986]. The apparent low sea surface temperatures during the Oxfordian could result from an erroneous estimate of the oxygen isotope composition of ambient seawater. A cooling stage could have been accompanied by the growth of a polar continental ice cap. The formation of a polar ice cap, even limited in size, could have led to a positive shift in the $\delta^{18}O$ of seawater in the Oxfordian relative to the Callovian. This change would be recorded in the $\delta^{18}O$ values of fish tooth enamel. The possible ice volume component of the $\delta^{18}O$ fish record cannot be simply determined without a knowledge concerning the extent of glacial sediments, the relative sea-level change, and the $\delta^{18}O$ value of Jurassic continental ice. However, basic calculations can provide first-order estimates. During Quaternary peak glacial times, most of the tropical surface temperatures cooled no more than 2–3°C with local exceptions around 5°C [e.g., *Broecker*, 1992]. Relative to the observed isotopic shift of 1.5‰ observed during early-middle Oxfordian, a $\delta^{18}O$ variation of 0.5‰ could be attributed to the ice volume component, assuming similar thermal variations for Jurassic and modern tropical surface waters. Considering an oxygen isotope composition for continental ice in the range −40 to −30‰, the mass of continental ice would range between 2×10^{19} kg and 3×10^{19} kg, and a fall in sea-level of about 50 m. *Dromart et al.* [2003] recently suggested the formation of polar ice to account for large-scale sea-level change, documented worldwide and of eustatic origin, with a maximum in the late Callovian. The geological evidence are (1) the occurrence of glendonites in the sediments of northern Asia, (2) deposition of deep-sea fans in Oman, (3) seaward migration of shorelines (North Sea), (4) valley incision in south Portugal and Saudi Arabia, and (5) subaerial exposures of marine sediments in Portugal, Israel, Alaska and Argentina. As noted by *Dromart et al.* [2003], the abrupt and global marine regression of the late Callovian follows the decrease of sea surface temperatures along with a southward migration of boreal ammonites. Therefore a glacial event is presented as a plausible scenario that could conciliate isotopic, paleontological and geological data.

[36] Similarly to biocarbonate systems, interpretation of the bioapatite $\delta^{18}O$ value in terms of temperature depends critically on the choice of the $\delta^{18}O$ seawater value. Our proposed temperatures may have to be revised, by probably less than three or four degrees, if independent evidence is found for a value other than 0‰ for $\delta^{18}O$ seawater. The

presence or absence of continental polar ice caps is a crucial element in this discussion. From a purely isotopic point of view for the period from the Bajocian through to the Thithonian (Figure 8), a tentative case can only be made for the presence of a significant continental ice reservoir during the Oxfordian, the Thithonian and perhaps the Bajocian-Bathonian, the three stages with relatively high $\delta^{18}O$ apatite values. These propositions are supported, in part, by the documented periods of major regression [*Guillocheau*, 1991; *Garcia et al.*, 1996] and occurrence of possible glacial phenomena in other part of the world [*Price*, 2000].

7. Conclusion

[37] Oxygen isotope compositions of marine vertebrate tooth enamel, that were not diagenetically altered, vary from 18.5 to 22.5‰ for the Middle-Late Jurassic of the western Tethyan basin. These data are interpreted as evidence for thermal variations of sea surface ($\leq$100 m) temperatures over a few Myr scale. A drop of isotopic temperatures (about 3°C to 5°C) occurred around the Callovian-Oxfordian boundary. This cooling of surface waters is associated with the southward migration of boreal ammonites and the development of temperate flora in the Anglo-Paris Basin. This cooler episode precedes a thermal increase that began during the late Oxfordian until the Kimmeridgian. Apparent isotopic temperatures not exceeding 20°C are low for tropical latitudes even when assuming an isotopic composition of seawater of 0‰ compatible with ^{18}O-enriched low-latitude sea surface waters and the absence of permanent well-developed polar ice caps. Therefore we cannot exclude the existence of an Oxfordian glaciation event that could explain the contemporaneous southward migration of boreal ammonites and the global sea-level fall.

[38] Strong oxygen isotope gradients (3‰) over 500 km from the northwest to the southeast of the basin suggest the development of a cool oceanic current during the middle-late Bathonian that could be related to the opening of the North Sea rift. According to paleontological and paleobotanical studies, we suggest that the late Callovian-early Oxfordian thermal decrease could be the expression of a global event rather than a more local geographic effect of these cool oceanic currents. In the absence of isotopic records provided by foraminifera, those available from fish phosphatic remains reveal that Jurassic climates were not so consistently warm and equable as previously thought.

[39] **Acknowledgments.** Sampling would not have been possible without the help of A. Prieur (Université Claude Bernard de Lyon), B. Laurin, J.-H. Delance (Université de Bourgogne), M. Weidmann (Université de Lausanne), A. Boullier (Université de Besançon), A. Léna, G. Gallio (Muséum de la Citadelle, Besançon), J. P. Goujon (MNHN, Paris), Muséum de Bâle, J. M. Mazin (Université de Poitiers), and G. Breton (Muséum du Havre), who provided some of the vertebrate samples. We also thank M. Emery for her help in sample analyses. The authors thank the reviewers David Dettman and Christina Hartman, who helped us to improve the scientific content of this manuscript. This work was supported by the CNRS through the programs "Intérieur de la Terre" (Comportement dynamique des plates-formes carbonatées) and "ECLIPSE."

References

Abbink, O., J. Targarona, H. Brinkhuis, and H. Visscher, Late Jurassic to earliest cretaceous palaeoclimatic evolution of the southern North Sea, *Global Planet. Change*, *30*, 231–256, 2001.

Adlis, D. S., E. L. Grossman, T. E. Ancey, and R. D. McLerran, Isotope stratigraphy and paleodepth changes of Pennsylvanian cyclical sedimentary deposits, *Palaios*, *3*, 487–506, 1988.

Bocherens, H., P. L. Koch, A. Mariotti, D. Geraads, and J. J. Jaeger, Isotopic biogeochemistry (C-13, O-18) of mammalian enamel from African Pleistocene hominid sites, *Palaios*, *11*, 306–318, 1996.

Broecker, W. S., *The Glacial World According to Wally*, 318 pp., Lahmont-Doherty Earth Observatory, Palisades, N. Y., 1992.

Brown, J., A. Colling, D. Park, J. Phillips, D. Rothery, and J. Wright, *Ocean Circulation*, 238 pp., Open Univ. Press, Milton Keynes, U. K., 1989.

Cappetta, H., Mesozoic and Cenozoic Elasmobranchii, in *Handbook of Paleoichtyology, Chondrichthyes II*, edited by H.-P. Schultze, pp. 193, Springer-Verlag, New York, 1987.

Cariou, E., D. Contini, J.-L. Dommergues, R. Enay, J. R. Geyssant, C. Mangold, and J. Thierry, Biogéographie des Ammonites et évolution structurale de la Téthys au cours du Jurassique, *Bull. Soc. Géol. Fr.*, *8*, 679–697, 1985.

Carpenter, S. J., and K. C. Lohmann, $\delta^{18}O$ and $\delta^{13}C$ values of modern brachiopod shells, *Geochim. Cosmochim. Acta*, *59*, 3749–3764, 1995.

Craig, H., and L. I. Gordon, Deuterium and oxygen-18 variations in the ocean and the marine atmosphere, in *Stable Isotopes in Oceanographic Studies and Paleotemperatures*, edited by E. Tongiorgi, pp. 9–130, Spoleto, Cons. Naz. delle Ric., Lab. di Geol. Nucl., Pisa, 1965.

Crowson, R. A., W. J. Showers, E. K. Wright, and T. C. Hoering, A method for preparation of phosphate samples for oxygen isotope analysis, *Anal. Chem.*, *63*, 2397–2400, 1991.

Cuny, G., Primitive neoselachian sharks: A survey, *Oryctos*, *1*, 3–21, 1998.

Davis, D. W., R. J. Sewell, and S. D. G. Campbell, U-Pb dating of Mesozoic igneous rocks from Hong Kong, *J. Geol. Soc. London*, *154*, 1067–1076, 1997.

Dercourt, J., L. P. Zonenshaim, L. P. Ricou, V. G. Kazmin, X. Le Pichon, and A. L. Knipper, Présentation de neuf cartes paléogéographiques au 1/20000000 s'étendant de l'Atlantique au Pamir pour la période du Lias à l'actuel, *Bull. Soc. Géol. Fr.*, *8*, 637–652, 1985.

Ditchfield, P. W., High northern palaeolatitude Jurassic-Cretaceous palaeotemperature variation: new data from Kong Karls Land, Svalbard, *Palaeogeogr. Palaeoclimatol. Palaeoecol.*, *130*, 163–175, 1997.

Dromart, G., P. Allemand, J.-P. Garcia, and C. Robin, Variation cyclique de la production carbonatée au Jurassique le long d'un transect Bourgogne-Ardèche, Est-France, *Bull. Soc. Géol. Fr.*, *167*, 423–433, 1996.

Dromart, G., J.-P. Garcia, S. Picard, F. Atrops, C. Lécuyer, and S. M. F. Sheppard, Ice age at the Middle-Late Jurassic transition?, *Earth Planet. Sci. Lett*, in press, 2003.

Féraud, G., V. Alric, M. Fornair, H. Bertrand, and M. Haller, $^{40}Ar/^{39}Ar$ dating of the Jurassic volcanic province of Patagonia: Migrating magmatism related to Gondwana break-up and subduction, *Earth Planet. Sci. Lett.*, *172*, 83–96, 1999.

Frakes, L. A., and J. E. Francis, Cretaceous palaeoclimates, in *Cretaceous Resources, Events and Rhythms*, edited by R. N. Ginsburg and B. Beaudoin, pp. 373–387, Kluwer Acad., New York, 1990.

Frakes, L. A., J. E. Francis, and J. I. Syktus, *Climate Modes of the Phanerozoic*, 274 pp., Cambridge Univ. Press, New York, 1992.

Garcia, J.-P., and G. Dromart, The validity of two biostratigraphic approaches in sequence stratigraphic correlations: Brachiopod zones and marker-beds in the Jurassic, *Sediment. Geol.*, *114*, 55–79, 1997.

Garcia, J.-P., G. Dromart, F. Guillocheau, P. Allemand, F. Gaumet, C. Robin, and G. Sambet, Bathonian-Callovian Paris Basin Subalpine Basin intercorrelations along an Ardennes-Ardèche cross-section, *C. R. Acad. Sci., Ser. II*, *323*, 697–703, 1996.

Gaumet, F., J.-P. Garcia, G. Dromart, and G. Sambet, Contrôle stratigraphique des faciès, géométries et profils de dépôt de la plate-forme carbonatée bourguignonne au Bathonien-Callovien, *Bull. Soc. Géol. Fr.*, *167*, 409–421, 1996.

Gonzalez, L. A., and K. C. Lohmann, Carbon and oxygen isotopic composition of Holocene reefal carbonates, *Geology*, *13*, 811–814, 1985.

Gradstein, F. M., F. P. Agterberg, J. G. Ogg, J. Hardenbol, P. Van Veen, J. Thierry, and Z. Huang, A Mesozoic time scale, *J. Geophys. Res.*, *99*, 24,051–24,074, 1994.

Guillocheau, F., Mise en évidence des grands cycles transgression-régression d'origine tecto-

nique dans les sédiments mésozoïques du Bassin de Paris, *C. R. Acad. Sci., Ser. II*, *312*, 1587–1593, 1991.

Gygi, R. A., and F. Persoz, Mineralostratigraphiy, litho- and biostratigraphiy combined in correlation of the Oxfordian (Late Jurassic) formations of the Swiss Jura range, *Eclogae Geol. Helv.*, *79*, 385–454, 1986.

Hallam, A., The determination of Jurassic environments using palaeoecological methods, *Bull. Soc. Géol. Fr.*, *169*, 681–687, 1998.

Hubbard, N. L. B., and M. C. Boulter, Mid Mesozoic floras and climates, *Palaeontology*, *40*, 43–70, 1997.

Iacumin, P., H. Bocherens, A. Mariotti, and A. Longinelli, Oxygen isotope analyses of coexisting carbonate and phosphate in biogenic apatite: A way to monitor diagenetic alteration of bone phosphate?, *Earth Planet. Sci. Lett.*, *142*, 1–6, 1996.

Kolodny, Y., and B. Luz, Oxygen isotopes in phosphates of fossil fish—Devonian to recent, in *Stable Isotope Geochemistry: A Tribute to Samuel Epstein*, edited by H. P. Taylor, J. R. O'Neil, and I. R. Kaplan, pp. 105–119, Geochem. Soc., San Antonio, Tex., 1991.

Kolodny, Y., and M. Raab, Oxygen isotopes in phosphatic fish remains from Israel: Paleothermometry of tropical Cretaceous and Tertiary shelf waters, *Palaeogeogr. Palaeoclimatol. Palaeoecol.*, *64*, 59–67, 1988.

Kolodny, Y., B. Luz, and O. Navon, Oxygen isotope variations in phosphate of biogenic apatites, I. Fish bone apatite-rechecking the rules of the game, *Earth Planet. Sci. Lett.*, *64*, 398–404, 1983.

Kolodny, Y., B. Luz, M. Sander, and W. A. Clemens, Dinosaur bones: Fossils or pseudomorphs?: The pitfalls of physiology reconstruction from apatitic fossils, *Palaeogeogr. Palaeoclimatol. Palaeoecol.*, *126*, 161–171, 1996.

Lécuyer, C., Oxygen isotope analysis of phosphates, in *Handbook of Stable Isotope Analytical Techniques*, Elsevier Sci., New York, in press, 2003.

Lécuyer, C., P. Grandjean, J. R. O'Neil, H. Cappetta, and F. Martineau, Thermal excursions in the ocean at the Cretaceous-Tertiary boundary (northern Morocco): The $\delta^{18}O$ record of phosphatic fish debris, *Palaeogeogr. Palaeoclimatol. Palaeoecol.*, *105*, 235–243, 1993.

Lécuyer, C., P. Grandjean, and C. C. Emig, Determination of oxygen isotope fractionation between water and phosphate from living lingulids: Potential application to palaeoenvironmental studies, *Palaeogeogr. Palaeoclimatol. Palaeoecol.*, *126*, 101–108, 1996a.

Lécuyer, C., P. Grandjean, F. Paris, M. Robardet, and F. Robineau, Deciphering "temperature" and "salinity" from biogenic phosphates: The $\delta^{18}O$ of coexisting fishes and mammals of the middle Miocene sea of western France, *Palaeogeogr. Palaeoclimatol. Palaeoecol.*, *126*, 61–74, 1996b.

Lécuyer, C., P. Grandjean, J. A. Barrat, C. C. Emig, J. Nolvak, F. Paris, and M. Robardet, $\delta^{18}O$ and REE contents of phosphatic brachiopods: A comparison between modern and lower Paleozoic populations, *Geochim. Cosmochim. Acta*, *62*, 2429–2436, 1998.

LeGeros, R. Z., and J. P. LeGeros, Phosphate minerals in human tissues, in *Phosphate Minerals*, edited by J. O. Nriagu and P. B. Moore, pp. 351–385, Springer-Verlag, New York, 1984.

Longinelli, A., and S. Nuti, Revised phosphate-water isotopic temperature scale, *Earth Planet. Sci. Lett.*, *19*, 373–376, 1973.

Marchand, D., and J. Thierry, Les influences mésogéennes et boréales dans le Callovien de Bourgogne, *Bull. Soc. Géol. Fr.*, *16*, 476–484, 1974.

Marchand, D., and J. Thierry, Enregistrement des variations morphologiques et de la composition des peuplements d'ammonites durant le cycle régressif/transgressif de 2ème ordre Bathonien inférieur-Oxfordien inférieur en Europe occidentale, *Bull. Soc. Géol. Fr.*, *168*, 121–132, 1997.

Martill, D. M., Predation on *Kosmoceras* by Semionotid fish in the middle Jurassic lower Oxford clay of England, *Paleontology*, *33*, 739–742, 1990.

McArthur, J. M., and A. Herczeg, Diagenetic stability of the isotopic composition of phosphate-oxygen: palaeoenvironmental implications, in *Phosphorite Research and Development*, edited by A. J. G. Notholt and I. Jarvis, pp. 119–124, Geol. Soc. Am., Boulder, Colo., 1990.

McCrea, J. M., On the isotopic chemistry of carbonates and a paleotemperature scale, *J. Chem. Phys.*, *18*, 849–857, 1950.

Michel, V., P. Ildefonse, and G. Morin, Chemical and structural changes in Cervus elaphus tooth enamels during fossilization (Lazaret cave): A combined IR and XRD Rietveld analysis, *Appl. Geochem.*, *10*, 145–159, 1995.

Morgans, H., S. P. Hesselbo, and R. A. Spicer, The seasonal climate of the Early-Middle Jurassic Cleveland Basin, England, *Palaios*, *14*, 261–272, 1999.

Nursall, J. R., Distribution and ecology of pycnodont fishes, in *Mesozoic Fishes 2- Systematics and Fossil Record*, edited by G. Arratia and H.-P. Schultze, pp. 115–124, F. Pfeil, Munich, 1996.

O'Neil, J. R., R. N. Clayton, and T. K. Mayeda, Oxygen isotope fractionation in divalent metal carbonates, *J. Chem. Phys.*, *51*, 5547–5558, 1969.

O'Neil, J. R., L. J. Roe, E. Reinhard, and R. E. Blake, A rapid and precise method of oxygen isotope analysis of biogenic phosphate, *Isr. J. Earth Sci.*, *43*, 203–212, 1994.

Philippe, M., and F. Thévenard, Distribution and paleoecology of the Mesozoic wood genus *Xenoxylon*: Palaeoclimatological implications for the Jurassic of western Europe, *Rev. Palaeobot. Palyno.*, *91*, 353–370, 1996.

Picard, S., J. P. Garcia, C. Lécuyer, S. M. F. Sheppard, H. Cappetta, and C. Emig, $\delta^{18}O$ values of coexisting brachiopods and fish: Temperature differences and estimates of paleowater depths, *Geology*, *26*, 975–978, 1998.

Podlaha, O. G., J. Mutterlose, and J. Veizer, Preservation of $\delta^{18}O$ and $\delta^{13}C$ in belemnite rostra from the Jurassic/Early Cretaceous successions, *Am. J. Sci.*, *298*, 324–347, 1998.

Poyato-Ariza, F. J., M. R. Talbot, M. A Fregenal-Martínez, N. Meléndez, and S. Wenz, First isotopic and multidisciplinary evidence for nonmarine coelacanths and pycnodontiform fishes: Palaeoenvironmental implications, *Palaeogeogr. Palaeoclimatol. Palaeoecol.*, *144*, 65–84, 1998.

Price, G., The evidence and implications of polar ice during the Mesozoic, *Earth Planet. Sci. Lett.*, *48*, 183–210, 2000.

Pucéat, E., C. Lécuyer, S. M. F. Sheppard, G. Dromart, S. Reboulet, and P. Grandjean, Thermal evolution of Cretaceous Tethyan marine waters inferred from oxygen isotope composition of fish tooth enamels, *Paleoceanography*, *18*(2), 1029, doi:10.1029/2002PA000823, 2003.

Riboulleau, A., F. Baudin, V. Daux, P. Hantzpergue, M. Renard, and V. Zakharov, Evolution de la paléotempérature des eaux de la plateforme russe au cours du Jurassique supérieur, *C. R. Acad. Sci., Ser. II*, *326*, 239–246, 1998.

Riding, J. B., and N. L. B. Hubbard, Jurassic (Toarcian to Kimmeridgian) dinoflagellate cysts and paleoclimates, *Palynology*, *23*, 15–30, 1999.

Robin, C., F. Guillocheau, P. Allemand, S. Bourquin, G. Dromart, J.-M. Gaulier, and C. Prijac, Echelles de temps et d'espace du contrôle tectonique d'un bassin flexural intracratonique: Le bassin de Paris, *Bull. Soc. Géol. Fr.*, *171*, 181–196, 2000.

Roth, P. H., Ocean circulation and calcareous nannoplankton evolution during the Jurassic and Cretaceous, *Palaeogeogr. Palaeoclimatol. Palaeoecol.*, *74*, 111–126, 1989.

Saelen, G., P. Doyle, and M. R. Talbot, Stable-isotope analyses of Belemnite rostra from the Whitby Mudstone Fm, England: Surface water conditions during deposition of a marine black shale, *Palaios*, *11*, 97–117, 1996.

Savin, S. M., The history of the Earth's surface temperature during the past 100 million years, *Ann. Rev. Earth Planet. Sci.*, *5*, 319–355, 1977.

Sharp, Z. D., V. Aturodei, and H. Furrer, The effect of diagenesis on oxygen isotope ratios of biogenic phosphates, *Am. J. Sci.*, *300*, 222–237, 2000.

Van Aarssen, B. G. K., R. Alexander, and R. I. Kagi, Higher plant biomarkers reflect palaeovegetation changes during Jurassic times, *Geochim. Cosmochim. Acta*, *64*, 1417–1424, 2000.

Veizer, J., et al., Oxygen isotope evolution of Phanerozoic seawater, *Palaeogeogr. Palaeoclimatol. Palaeoecol.*, *132*, 159–172, 1997.

Vennemann, T. W., and E. Hegner, Oxygen, strontium, and neodymium isotope composition of fossil shark teeth as a proxy for the palaeoceanography and palaeoclimatology of the Miocene northern Alpine Paratethys, *Palaeogeogr. Palaeoclimatol. Palaeoecol.*, *142*, 107–121, 1998.

Vennemann, T. W., E. Hegner, G. Cliff, and G. W. Benz, Isotopic composition of recent shark teeth as a proxy for environmental conditions, *Geochim. Cosmochim. Acta*, *65*, 1583–1599, 2001.

Vidier, J.-P., J.-P. Garcia, J. Thierry, and D. Fauconnier, Le Dogger du Boulonnais: Nouveaux découpages chronologiques et séquentiel des formations carbonatées jurassiques en bordure du massif Londres-Brabant, *C. R. Acad. Sci., Ser. II*, *320*, 219–226, 1995.

Ziegler, P. A., Evolution of the Artic-North Atlantic and the western Tethys, *Am. Assoc. Petrol. Geol. Mem.*, *43*, 198, 1988.

G. Dromart, P. Grandjean, C. Lécuyer, and S. Picard, Laboratoire Paléoenvironnements et Paléobiosphère, CNRS UMR 5125, Campus de la Doua, Université Claude Bernard Lyon 1, F-69622 Villeurbanne, France.(Gilles.Dromart@univ-lyon1.fr; Patricia.Grandjean@univ-lyon1.fr; clecuyer@univ-lyon1.fr; Stephanie.Picard@univ-lyon1.fr)

J.-P. Garcia, Centre des Sciences de la Terre, CNRS UMR 5561, Université de Bourgogne, 6 Boulevard Gabriel, F-21000 Dijon, France. (Jean-Pierre.Garcia@u-bourgogne.fr)

S. M. F. Sheppard, Laboratoire de Sciences de la Terre, CNRS UMR 5570, Ecole Normale Supérieure de Lyon, 46 allée d'Italie, F-69364 Lyon, France. (simon.sheppard@ens-lyon.fr)